Research paper

Highly active and selective Au thin layer on Cu polycrystalline surface prepared by galvanic displacement for the electrochemical reduction of CO$_2$ to CO

Jun-Hyuk Kim [a,b,1], Hyunje Woo [b,1], Su-Won Yun [a], Hyun-Woo Jung [a], Seoin Back [c], Yousung Jung [c,*], Yong-Tae Kim [a,*]

[a] School of Mechanical Engineering, Pusan National University, Busan 46241, Republic of Korea
[b] Hybrid Materials Solution National Core Research Center (NCRC), Pusan National University, Busan 46241, Republic of Korea
[c] Graduate School of EEWS, Korea Advanced Institute of Science and Technology (KAIST), Daejeon 34141, Republic of Korea

ARTICLE INFO

ABSTRACT

An electrochemical reduction of CO$_2$ to CO has become a challenging issue in CO$_2$ utilization in order to mitigate the climate change. In this study, we report a promising approach to prepare Au-based electro-catalysts for the electrochemical reduction of CO$_2$ to CO having the maximized activity/selectivity and the minimized Au usage. It was clearly confirmed that the Au thin layer formed by the electrochemical galvanic displacement on polycrystalline Cu surface resulted in a markedly enhanced performance for the electrochemical reduction of CO$_2$ to CO. The CO Faradaic efficiency for the Au thin layer on Cu was 10.6 and 3.4 times higher than that for the polycrystalline Cu and Au, respectively. It was revealed from the photoemission spectroscopy (PES) studies that the increase of electron population in s-band and the upshift of d-band center position of Au in Au/Cu increased the bond strength with reaction intermediates leading to the enhancement of activity and the selectivity. Along with the electronic effect, the geometric effect like the increased the electrochemical surface area (ECSA) and proportion of low coordinated sites also played a substantial role in the performance enhancement.

© 2017 Elsevier B.V. All rights reserved.

1. Introduction

An effective conversion of CO$_2$ to CO can help in the reduction of CO$_2$ concentration to mitigate a radical climate change and in the production of synthesis gas (syngas) being used as feedstock in various chemical industries. For this purpose, one of the most common approaches is the electrochemical reduction of CO$_2$. To date, various metals such as Cu [1], Pb [2], Sn [3], Ag [4], and Au [5–7] have been examined for the electrochemical reduction of CO$_2$, but most of tested metals unfortunately showed the evolution of a large amount of H$_2$ rather than CO, showing a low selectivity [8]. Among them, Au exhibited extraordinarily higher activity and selectivity than other metals, even though it is inevitable to increase the manufacturing cost [8].

Several previous studies on the electrochemical reduction of CO$_2$ with various types of Au like Au nanopaticles [5] or Au oxide

[6] have been reported. Recently, Norskov et al. demonstrated an activity descriptor for CO$_2$ electroreduction [9,10], and subsequently, Yang et al. demonstrated the enhanced activity and selectivity for CO$_2$ electroreduction with well-controlled Au-Cu bimetallic nanoparticles [11]. They reported that the high activities of Au$_3$Cu resulted from electronic and geometric effects. However, few studies have been reported to understand the electronic structure change of Au by the interaction with Cu in details.

In this study, we tried to prepare Au thin layers on polycrystalline Cu, in which the thickness was controlled in order to maximize the electronic interaction in the interface between two kinds of metals. An electrochemical galvanic displacement method which was well-known approach to prepare noble metal skin on less noble metal substrate was employed to prepare the Au thin layer on Cu polycrystalline surface. In particular, we found a favorable charge transfer and d-band center shift for the electrochemical reduction of CO$_2$ through the XPS analysis, which provided us a clue to understand the mechanism of enhanced activity and selectivity for Au thin layer on Cu.

* Corresponding authors.
E-mail addresses: ysjn@kaist.ac.kr (Y. Jung), yongtae@pusan.ac.kr (Y.-T. Kim).
[1] These authors contributed equally to this work.

2. Experimental

2.1. Catalyst fabrication

The Au skin on Cu (Au/Cu) catalyst was fabricated using a polycrystalline Cu pellet (diameter and height of 1/4'' each, 99.99% purity). The polycrystalline Cu was mechanically polished with #600/P1200, #800/P1500, and #1200/P2500 sand paper (silicon carbide, MICROCUT®, BUEHLER) to obtain a clean surface, which was then polished with alumina (0.05 μm). The prepared Cu was sonicated for several minutes, rinsed thoroughly with triple distilled water, and carefully dried at room temperature. Subsequently, the Cu was placed in a quartz chamber with Ar flow for 15 min and then annealed using an induction heater (AMBRELL, HOTSHOT 2 Ext.FF V4) at ~800 °C for 300 s under Ar/H$_2$ flow (5% hydrogen). The heat-treated Cu was cooled to room temperature for 10 min under Ar flow to eliminate any H$_2$ gas. Subsequently, a 0.01 mM solution of AuCl$_3$ in H$_2$SO$_4$ was sequentially dropped onto the surface of Cu, and the Cu with AuCl$_3$ was stored for 30 min, 60 min, and 180 min under Ar flow to carry out Au galvanic displacement. For comparison, polycrystalline Au and Cu were prepared.

2.2. Characterization

The morphology of the catalysts was determined using scanning electron microscopy (SEM, Zeiss FE-SEM SUPRA25 and Raith Quantum Elphy) and energy dispersive X-ray spectroscopy (EDS, Ametek, Apollo X, LN2 free type). For atomic force microscopy (AFM) studies, the samples were fixed on sticky carbon tape and measurement was carried out using a XE-100 model operating in contact mode. The high-resolution photoemission spectroscopy (HR-PES) study was performed at the 8A2 (HR-PES II) undulator beam-line of the Pohang Accelerator Laboratory (PAL) in Korea with photon energies of 630 and 130 eV for core-level and valence band studies, respectively. This beam-line is equipped with an electron analyzer (SES100, Gamma Data Scienta). The chamber was maintained at room temperature with a background pressure of less than 1×10^{-10} Torr during the measurements. The samples were attached using carbon tape before being introduced into the chamber. A three-electrode electrochemical cell on a potentiostat (Biologic VSP) was used for electrochemical measurements. The catalysts were used as the working electrode. An Ag/AgCl in saturated NaCl electrode converted to the reversible hydrogen electrode (RHE) scale and a high surface area platinum mesh were used as the reference and counter electrode, respectively. All electrochemical tests were carried out in a CO$_2$-saturated electrolyte (0.1 M KHCO$_3$, Sigma-Aldrich, 99.99% metals basis) at 1600 rpm in order to minimize bubble blockage on the electrode surface. The pH of the CO$_2$-saturated electrolyte was measured to be 6.8. During chronoamperometry (CA), the exit gas from the home-made fully sealed cell was passed through the sampling loop of a gas chromatograph (GC, YL6500) and analyzed after 5 min to quantify the gas-phase products. The liquid products were analyzed by ^{1}H nuclear magnetic resonance (NMR) spectroscopy using a Unity-Inova 500 (500 MHz) spectrometer. The working and reference electrodes were separated from the counter electrode using a membrane (Nafion 212, Dupont) to minimize the effect of the oxidizing gas produced at the counter electrode.

3. Results and discussion

The thickness of Au was controlled by the immersion time (30, 60 and 180 min) of Cu surface into solution containing Au precursors (Fig. S1 and Fig. 1). The sample with Au galvanic displacement for 180 min showed thicker nanostructure of Au. The Au thin layer on Cu (denoted by Au/Cu in this paper) prepared by 60 min immersion showed the best CO faraday current (Fig. S2 and S3) and therefore was mainly examined to understand the electronic interaction between Au and Cu with various analysis tools. Fig. 1 shows the morphology of the Au/Cu catalysts prepared by 60 min (a), and the polycrystalline Cu and Au (b). Both the polycrystalline Cu and Au have smooth flat surfaces with tiny scratches in the same directions that is attributed to the trace of mechanical polishing in the sample preparation process. The Au/Cu catalyst had a compact boundary arrangement of the Au microstructure layer with tiny grains (~30 nm) on polycrystalline Cu and a vertical thickness was observed to be about 20 nm with Au/Cu lamella structure. EDX analysis clearly revealed that Au was uniformly distributed on the Cu surface (EDX details are presented in Fig. S4). The spot in selected area electron diffraction pattern, corresponding to a satisfied diffraction condition of the sample's crystal structure, show that the measured interspacing (d = 0.235 nm) was well consistent with Au (111), as shown in Fig. 1c.

The CO$_2$ electrochemical reduction performances of polycrystalline Cu, Au as well as the Au/Cu catalyst were evaluated by linear sweep voltammetry (LSV), as shown in Fig. 2a. All samples were tested under the same electrochemical condition with an
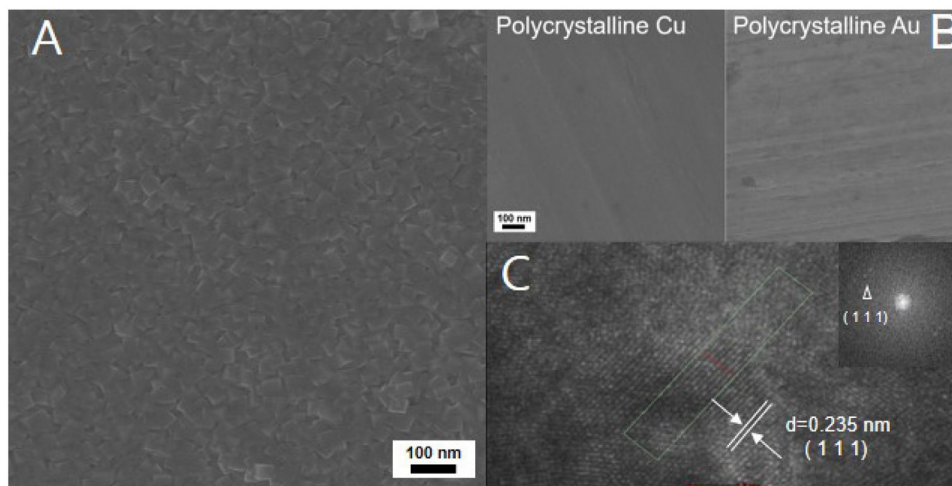

Fig. 1. (a) SEM images of Au/Cu catalyst, (b) polycrystalline Cu (left) and Au (right). (c) HRTEM image of close-up Au in Au/Cu with corresponding selected area electron diffraction pattern of (1 1 1) at the inset.
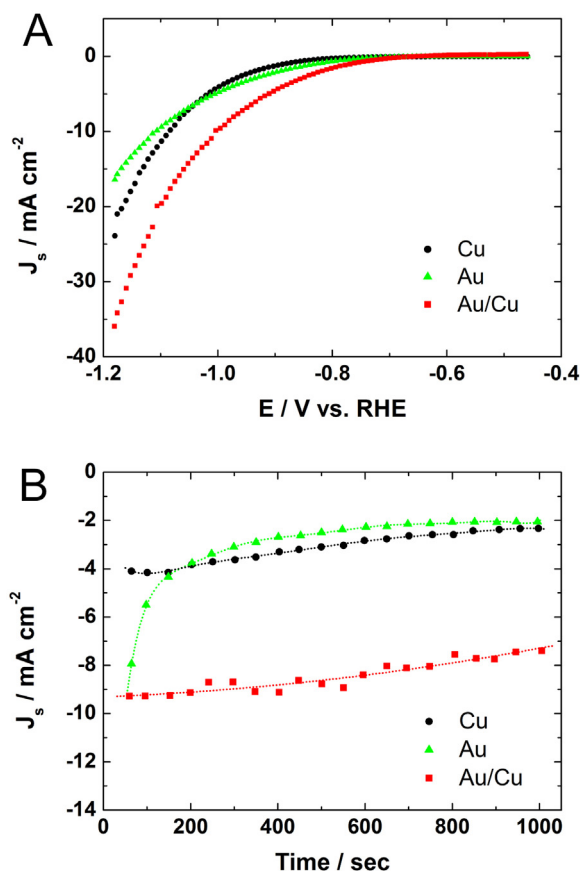
Fig. 2. (A) Total current density plot and (B) chronoamperometric curves in terms of current densities of polycrystalline Cu and Au as well as the Au/Cu catalyst.
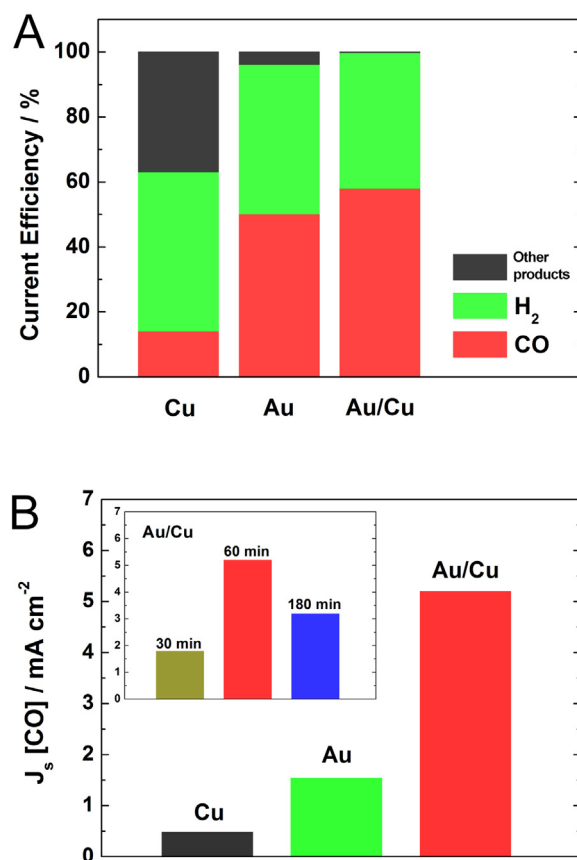
Fig. 3. (A) Faradaic current efficiency of CO_2 reduction distribution for CO and H_2; (B) CO current density of polycrystalline Cu and Au as well as the Au/Cu catalyst at −1.0 V vs. RHE. The inset, CO faradaic current efficiency of galvanic displaced Au/Cu for 30 min, 60 min and 180 min, is included for comparison.

i-R compensation. Au had a slightly higher activity in the lower overpotential range (from −1.0 V to −0.4 V), but its current density became lower than that of Cu at higher overpotential range (from −1.2 V to −1.0 V). The current density of Cu at −1.0 V was 4.5 mA/cm^2, which is close to the previously measured current density of approximately 5 mA/cm^2 [1]. It is interesting to note that the current density was much higher for Au/Cu than other samples, with a current density of more than 35 mA/cm^2 at −1.2 V. However, this does not assure that Au/Cu has superb CO_2 reduction activity, because this current density includes a substantial contribution of the hydrogen evolution reaction (HER) from the dissociation of water, a competing reaction in the aqueous electrolyte.

In order to distinguish the two main origin of obtained current density for Au/Cu, we adopted a CA with a GC anaylsis, as shown in Fig. 2b. It is widely recognized that at higher overpotential range (above −1.18 V), the cell temperature rose with time along with a decrease in the solubility of CO_2, causing fluctuations in current density [1]. To avoid noisy data caused by vigorous evolution of bubbles blocking the electrode surface, we chose a potential of −1.0 V for the CA analysis. CO_2 was fully saturated before the test with the flow rate of 20 ml/min maintained during the experiment. Since the electrochemical surface area (ECSA) can be changed owing to the formation and/or elimination of bubbles, it was hard to determine an exact solution resistance for i-R compensation, as reported previously [1]. With this reason, a constant current density without any fluctuation could not be obtained in the reaction time, but the obtained data are good enough to understand the tendency of current density variation in various samples. At 300 s, the current densities of Cu and Au were found to be 3.6 mA/cm^2 and 3.1 mA/cm^2, respectively, while that of Au/Cu (9.0 mA/cm^2) was much higher than the other samples.

GC data were obtained by capturing product gases at 300 s during the CA tests, as shown in Fig. 3. The plot shows that H_2 and CO are the major products in the electrochemical reduction of CO_2 using Au and Au/Cu, while the polycrystalline Cu produced chiefly H_2 and other products including formate, methanol and various short organic carbon rather than CO. The sum of the Faradaic yield for all products approached 100%. In the case of Cu, the current efficiency for hydrogen production was found to be 49%. It is well consistent with the previous report, where the H_2 current efficiency was closely 40%, while that for CO production was only 14% [12]. On the other hand, the polycrystalline Au showed the current efficiency of 50% for HER, 46% for CO production, and only 4% for other products. Interestingly, the Au/Cu demonstrated a better performance than other samples in spite of much lower Au usage, showing that the current efficiencies for CO, H_2, and formats were 58%, 41%, and 1%, respectively. Faraday efficiency of formate synthesized by Au/Cu catalyst was obtained by NMR spectroscopy (Fig. S5). Based on this electrochemical and GC analysis, the partial current density for CO production can be calculated as shown in Fig. 3b. At a potential of −1.0 V, the current density for only CO production for Au (1.55 mA/cm^2) was 3.2 times higher than that for Cu (0.49 mA/cm^2), respectively. Moreover, the current density for Au/Cu (5.21 mA/cm^2) was 3.4 times higher than that for the polycrystalline Au. Also, we performed the stability tests for Au/Cu catalyst. The current density was maintained during 6 h, showing high stability of Au/Cu catalyst for CO_2 electro-reduction (Fig. S6). The pH value was the same for 8 h without marked decrease or increase (Fig. S7). These results indicate that the Au thin layer on Cu can achieve the enhancement of activity, selectivity and stability
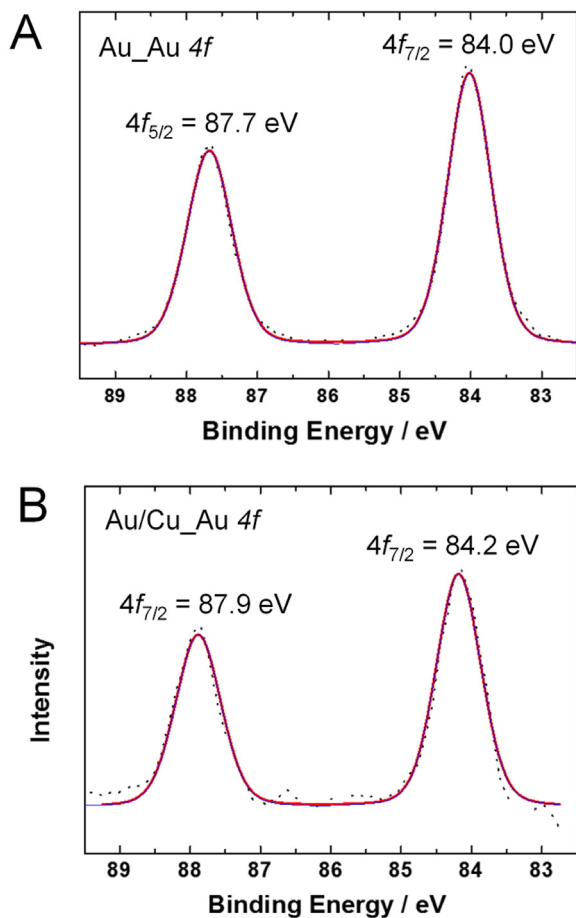
Fig. 4. XPS Au 4f core level signals of (A) polycrystalline Au and (B) the Au/Cu catalyst recorded at the 8A2 beam-line of Pohang Accelerator Laboratory (PAL). The dotted line and solid red line represent raw measured data and the fitted curves, respectively. (For interpretation of the references to colour in this figure legend, the reader is referred to the web version of this article.)

Table 1
XPS details of the elemental composition of the Au, Au/Cu, and Cu catalysts. The peaks corresponding to Au 4f and Cu 3p have been analyzed.

Core levels	Au	Au/Cu	Cu
Au $4f_{7/2}$	84.0 eV	84.2 eV	–
Au $4f_{5/2}$	87.7 eV	87.9 eV	–
Cu $3p_{3/2}$	–	75.1 eV	75.1 eV
Cu $3p_{1/2}$	–	77.3 eV	77.3 eV

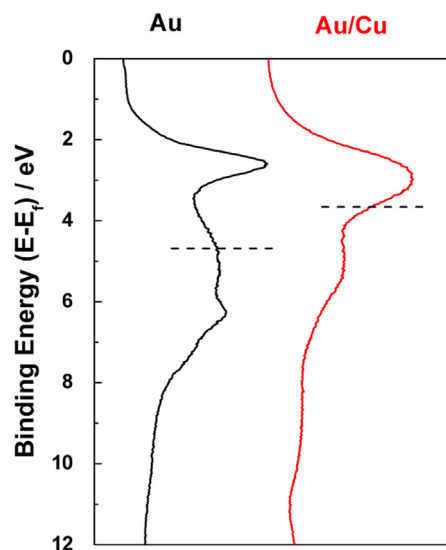**Fig. 5.** Valence band spectra of polycrystalline Au and Au/Cu recorded at the 8A2 beam-line PAL with a photon energy of 130 eV.

for the electrochemical reduction of CO_2 to CO with a minimized Au usage.

It is widely recognized that the binding strength of an adsorbate atom to the catalyst surface is the most critical factor in determining the efficiency of CO_2 reduction [9,10,13,14]. We have, therefore, investigated the electronic structure of samples, mainly core levels and valence bands which are directly related to the adsorption strength, in order to understand the underlying reason for the higher CO production efficiency for the Au/Cu catalyst. When a metal surface comes into contact with another metal or oxide surface, a charge transfer is induced because of the difference in the electronic environment [15–19]. Therefore, the electronic state of surfaces is considered to be a key factor to determine the adsorption behavior [20].

A PES was employed in order to investigate the electronic state of surfaces. The PES spectra were obtained by using the synchrotron beam at Pohang Light Source (PLS), as can be seen in Fig. 4. All raw data were calibrated with Au 4f at a binding energy of 84 eV of a separated Au foil as a reference. A data fitting was performed after Shirley background subtraction from 82.5 to 89.5 eV for Au to eliminate the spectral background originating from inelastically scattered electrons [21] and the fitting results for Au, Au/Cu, and Cu were summarized in Table 1. The Au $4f_{7/2}$ peak for polycrystalline Au was shown at 84.0 eV which is well consistent with the literature value [22], while that for Au/Cu was shifted to a higher binding energy (84.2 eV). This core peak shift is agreed with the

previous report for the Au-Cu alloy system [23], in which Eberhardt et al. showed that the charge overcompensation due to the decrease of sd-hybridization can lead to the shift of Au $4f_{7/2}$ binding energy to higher energy, even though the population of sp-band is rather increased by the charge transfer from Cu to Au. It is widely recognized that the increase of electron population in sp-band strengthens the chemical bond between metal surfaces and adsorbates, because the repulsion force between them is decreased by an enlarged bond length [15,24]. Hence, the Au thin layer on Cu can have higher adsorption strength with reaction intermediates. For the Cu core level, Au deposition did not cause a shift, and the Cu 3p level was remained the same as that in polycrystalline Cu and Au/Cu (Cu 3p spectra are shown in Fig. S8), which can be attributed to the bulk Cu substrate in Au/Cu.

Investigation of the valence band also provides specific information about the change in electronic structure. The observed valence band shift of Au/Cu provides clear evidence of electronic structure modification. Fig. 5 shows the valence band spectra of Au and Au/Cu, where the positions of the d-band center can be calculated. It is obvious that the d-band center position for Au/Cu is closed to the Fermi level ($E_F = 0$) and higher than that for Au. According to the experimentally observed CO_2 reduction trends reported by the Norskov group [10], the Au sits atop the optimal state for CO_2 reduction but still requires a significant overpotential step to proceed reduction from CO_2 to COOH. Therefore, one of the strategies for enhanced CO_2 reduction is to increase the bond strength of CO modifying slightly the nature binding energy of pure Au, which can make the dissociation of CO_2 to COOH more efficiently. The shift of d-band center position could also change the binding geometry of the adsorbate. Norskov et al. asserts that a correlation (so called scaling relation) exists between the d-band center position and the adsorption energies with CO [25]. When the d-band center of Au moves upwards (close to the Fermi level), the bond strength of CO

becomes stronger. This can be a primary clue to understanding the enhanced conversion performance of Au/Cu. Based on these results, we suggest that by fabricating the Au thin film on Cu, the electronic structure of Au can be tuned to strengthen the bond with CO and eventually enhance the activity for electrochemical reduction of CO_2 to CO.

Along with the change of electronic structure, a geometric effect like ECSA or a proportion of low coordinated sites can be also considered as another origin of the enhanced activity and selectivity of Au/Cu. The ECSA was measured from the measurements of the double-layer capacitance [26], as shown in Fig. S9. The ECSA of Au/Cu ($25.2\,cm^2$) was much higher than that of polycrystalline Cu ($0.7\,cm^2$) and Au ($2.48\,cm^2$). The high value of ECSA for Au/Cu can be attributed to Au tiny grains formed under the galvanic displacement process. The tiny grains must have much higher proportion of low coordinated sites than the smooth polycrystalline surface. It is already verified that the low coordinated sites like edge, corner or kink show a higher selectivity than the crystal plane for electrochemical reduction of CO_2 to CO [6,27,28]. Hence, we can conclude that the increase of ECSA and proportion of low coordinated sites is another origin of the enhanced activity and selectivity for Au/Cu.

In summary, the Au thin layer on Cu catalyst was successfully fabricated by using the galvanic displacement approach. From the core level study with PES, it was revealed that s electron charge was transferred from Cu to Au, which increased the bond strength with the adsorbate. Furthermore, the valence band analysis clearly confirmed that the d-band center position for Au/Cu was shifted upwards close to EF. This electronic structure change led to the enhanced activity and selectivity for electrochemical reduction of CO_2. As well as the electronic effect, the geometric effect like the increased ECSA and proportion of low coordinated sites also played a substantial role in the performance enhancement. Hence, it is concluded that the galavanic displacement to form the Au thin layer on Cu is a promising approach to prepare the electrocatalysts for electrochemical reduction of CO_2 to CO, with a minimized Au usage.

Acknowledgments

Appendix A. Supplementary data

Supplementary data associated with this article can be found, in the online version, at http://dx.doi.org/10.1016/j.apcatb.2017.05.001.

References

[1] K.P. Kuhl, E.R. Cave, D.N. Abram, T.F. Jaramillo, Energy Environ. Sci. 5 (2012) 7050–7059.
[2] C.H. Lee, M.W. Kanan, ACS Catal. 5 (2015) 465–469.
[3] Y.H. Chen, M.W. Kanan, J. Am. Chem. Soc. 134 (2012) 1986–1989.
[4] T. Hatsukade, K.P. Kuhl, E.R. Cave, D.N. Abram, T.F. Jaramillo, Phys. Chem. Chem. Phys. 16 (2014) 13814–13819.
[5] W. Zhu, R. Michalsky, Ö. Metin, H. Lv, S. Guo, C.J. Wright, X. Sun, A.A. Peterson, S. Sun, J. Am. Chem. Soc. 135 (2013) 16833–16836.
[6] Y. Chen, C.W. Li, M.W. Kanan, J. Am. Chem. Soc. 134 (2012) 19969–19972.
[7] W. Zhu, Y.-J. Zhang, H. Zhang, H. Lv, Q. Li, R. Michalsky, A.A. Peterson, S. Sun, J. Am. Chem. Soc. 136 (2014) 16132–16135.
[8] Y. Hori, Electrochemical CO_2 Reduction on Metal Electrodes: Modern Aspects of Electrochemistry, Springer, New York, 2008, pp. 89–189.
[9] H.A. Hansen, J.B. Varley, A.A. Peterson, J.K. Nørskov, J. Phys. Chem. Lett. 4 (2013) 388–392.
[10] A.A. Peterson, J.K. Nørskov, J. Phys. Chem. Lett. 3 (2012) 251–258.
[11] D. Kim, J. Resasco, Y. Yu, A.M. Asiri, P. Yang, Nat. Commun. 5 (2014).
[12] S. Sen, D. Liu, G.T.R. Palmore, ACS Catal. 4 (2014) 3091–3095.
[13] C. Liu, T.R. Cundari, A.K. Wilson, J. Phys. Chem. C 116 (2012) 5681–5688.
[14] L. Liu, C. Zhao, Y. Li, J. Phys. Chem. C 116 (2012) 7904–7912.
[15] J.-H. Kim, S. Chang, Y.-T. Kim, Appl. Catal. B 158–159 (2014) 112–118.
[16] P. Liu, J.K. Norskov, Phys. Chem. Chem. Phys. 3 (2001) 3814–3818.
[17] J.A. Rodriguez, D.W. Goodman, Science 257 (1992) 897–903.
[18] V.R. Stamenkovic, B. Fowler, B.S. Mun, G. Wang, P.N. Ross, C.A. Lucas, N.M. Marković, Science 315 (2007) 493–497.
[19] P. Strasser, S. Koh, T. Anniyev, J. Greeley, K. More, C. Yu, Z. Liu, S. Kaya, D. Nordlund, H. Ogasawara, M.F. Toney, A. Nilsson, Nat. Chem. 2 (2010) 454–460.
[20] W. Tang, G. Henkelman, J. Chem. Phys. 130 (2009) 194504.
[21] B.S. Mun, M. Watanabe, M. Rossi, V. Stamenkovic, N.M. Markovic, P.N. Ross, J. Chem. Phys. 123 (2005) 204717.
[22] S. Hüfner, G.K. Wertheim, Phys. Rev. B 11 (1975) 678–683.
[23] W. Eberhardt, S.C. Wu, D. Garrett, D. Sondericker, F. Jona, Phys. Rev. B 31 (1985) 8285–8287.
[24] H. Xin, A. Holewinski, N. Schweitzer, E. Nikolla, S. Linic, Top. Catal 55 (2012) 376–390.
[25] J.K. Nørskov, F. Abild-Pedersen, F. Studt, T. Bligaard, Proc. Natl. Acad. Sci. 108 (2011) 937–943.
[26] C.C.L. McCrory, S. Jung, J.C. Peters, T.F. Jaramillo, J. Am. Chem. Soc. 135 (2013) 16977–16987.
[27] W. Zhu, R. Michalsky, O.¨ Metin, H. Lv, S. Guo, C.J. Wright, X. Sun, A.A. Peterson, S. Sun, J. Am. Chem. Soc. 135 (2013) 16833–16836.
[28] W. Zhu, Y.-J. Zhang, H. Zhang, H. Lv, Q. Li, R. Michalsky, A.A. Peterson, S. Sun, J. Am. Chem. Soc. 136 (2014) 16132–16135.